

**Slipping past UGT1A1 and Mrp2 in the liver. Effects of steric compression and hydrogen bonding on the hepatobiliary elimination of synthetic bilirubins.**

Antony F. McDonagh, Stefan E. Boiadjiev, and David A. Lightner

Division of Gastroenterology and The Liver Center, University of California San Francisco, San Francisco, California (A.F.McD)

Department of Chemistry, University of Nevada, Reno, Nevada (S.E.B., D.A.L.)

- a) **Running Title:** Steric compression, H-bonding and biliary excretion of bilirubins.
- b) **Corresponding Author:**  
Antony F. McDonagh  
Division of Gastroenterology and The Liver Center  
Room S-357. Box 0538  
University of California San Francisco  
San Francisco, CA 94143-0538  
Email: tony.mcdonagh@ucsf.edu
- c) **Number of Text Pages:** 22  
**Number of Tables:** 1  
**Number of Figures:** 16  
**Number of References:** 29  
**Words in the Abstract:** 202  
**Words in Introduction:** 719 (references not included), 813 (references included)  
**Words in Discussion:** 1195 (references included)
- d) **Abbreviations:** **MeDocta**, 0.1 M di-*n*-octylamine acetate in MeOH; **MRP2 (Mrp2)** , multidrug resistance-associated protein 2; **TR<sup>-</sup>**, Mrp2-deficient.

## Abstract

The hepatobiliary metabolism and excretion of three isomeric bilirubin analogs with propanoic replaced by benzoic acid side-chains were studied in the rat. Despite their isomeric relationship and similar constitutions, the three analogs were metabolized quite differently from each other and from bilirubin. In the di-*o*-benzoic compound, steric hindrance involving the phenyl groups reinforces intramolecular hydrogen bonding of the two carboxyl groups. This compound is considerably less polar than bilirubin on reverse-phase HPLC and, like bilirubin, was not excreted in bile in UGT1-deficient (Gunn) rats. But, quite unlike bilirubin, it was not glucuronidated or excreted in bile in normal rats. In contrast to both bilirubin and the di-*o*-benzoic isomer, the more polar *m*- and *p*-isomers, in which intramolecular hydrogen bonding of carboxyl groups is sterically difficult, were excreted rapidly in bile in unchanged form in both normal and Gunn rats. However, only one of them, the di-*m*-isomer, was excreted rapidly and unchanged in bile in rats (TR<sup>-</sup> rats) congenitally-deficient in the canalicular ABC transporter Mrp2. The marked differences in hepatobiliary metabolism of the three isomers studied can be rationalized on the basis of their computed three-dimensional structures and minimum-energy conformations and the remote effects of steric compression on intramolecular hydrogen bonding.

Bilirubin (**1**) is formed in mammals by reduction of biliverdin (**2**), end product of most heme catabolism. It is insoluble in water, lipophilic, extensively protein-bound in plasma and, unlike biliverdin, requires Phase 2 metabolism, mainly to mono and diglucuronides, for elimination. Once used as a liver function test (Harrop and Barron, 1931; Kornberg, 1942), bilirubin is a constituent of several Asian traditional medicines (McDonagh, 1990) and its antioxidant/anti-inflammatory properties are attracting current attention (Stocker et al., 1987; Stocker, 2004; Ollinger et al., 2007a; Ollinger et al., 2007b). Historically, bilirubins have been useful for investigating mechanisms of acyl glucuronidation, membrane transport and hepatobiliary excretion. Bilirubin and its two monoglucuronides are isozyme-specific substrates for the glucuronosyl transferase UGT1A1 (Owens et al., 2005), and its three acyl glucuronides are classic examples of compounds that depend wholly on the ABC transporter MRP2 (ABCC2) for elimination in bile (Nies and Keppler, 2007). Deficiencies of UGT1A1 cause neonatal jaundice, Gilbert's and Crigler-Najjar syndromes (Kaplan and Hammerman, 2005), and congenital deficiency of MRP2 underlies the rare Dubin-Johnson syndrome (Nies and Keppler, 2007). Studies on bilirubin glucuronides led to the discovery that acyl glucuronides of many drugs are reactive, potentially toxic, metabolites (Smith et al., 1986), and studies on bilirubin analogs have revealed how subtle changes in molecular conformation can profoundly influence hepatic metabolism (McDonagh and Lightner, 1991; McDonagh et al., 2001; McDonagh and Lightner, 2007). Thus, while not generally considered as drugs, bilirubins are insightful models for studying many aspects of drug metabolism.

Although often depicted as in **1**, bilirubin is not linear (Person et al., 1994). It is conformationally mobile and tends to adopt chiral conformations that are stabilized by intramolecular hydrogen bonding between the carboxyl (or carboxylate) groups and juxtaposed NH and NHCO functions (**Fig 2**). Such "ridge-tile" conformers occur in crystalline bilirubin and its salts, in solution, and probably in bilirubin serum-albumin complexes. Their predominance seems to dictate bilirubin's metabolism. Minor modifications of the alkyl side-chains have little effect on metabolism, but structural modifications that

prevent or stress the intramolecular hydrogen bonding have a marked effect. Thus, conversion of either of the two *Z* double bonds at C4-C5 and C15-C16 to the corresponding *E* configuration generates isomers that do not require glucuronidation for excretion in bile in rats or humans, a reaction that is clinically important in phototherapy of neonatal jaundice (Lightner and McDonagh, 1984). Separating the dipyrromethenone chromophores by inserting spacers in place of the central C10 bridge, as in **3** and **4**, also leads to molecules that do not require Phase 2 metabolism for facile biliary elimination (McDonagh et al., 2001; McDonagh and Lightner, 2007). And molecules, such as **5**, that represent one half of a bilirubin molecule and do not contain NH/NHCO functions to which the lone COOH can reach are also eliminated largely unchanged in bile in the rat (McDonagh and Lightner, 1991). Recent studies on exploded bilirubins containing linear acetylene linkages between the chromophores provide further evidence for the decisive role of hydrogen bonding and conformation in their metabolism (McDonagh and Lightner, 2007).

More subtle, superficially minor, structural changes can also influence the hydrogen bonding with major effects on metabolism (McDonagh and Lightner, 2007). Mesobilirubin XIII $\alpha$  (**6b**) is metabolized in the rat identically to bilirubin and eliminated in bile as a mono and a diglucuronide. Extension of each propanoic acid side-chain by one carbon gives a pigment (**6c**) that behaves similarly. But shortening the side-chains by just one carbon each (**6a**), or lengthening them by two or three carbons (**6d,e**) gives pigments that no longer require conjugation for elimination and are excreted unchanged in bile when administered to rats (Gunn rats) deficient in UGT1A isozymes. Such marked differences in metabolism are difficult to explain on the basis of linear representations like **6**, but are consistent with the calculated preferred three-dimensional structures of the molecules.

In higher homologs of **6**, with  $n = 4$  or  $5$ , non-bonded interactions involving CH<sub>2</sub> groups of the flexible alkanolic acid side-chains begin to become significant and perturb the tight hydrogen-bonding that is possible when  $n = 2$  or  $3$  (Trull et al., 1997; McDonagh and Lightner, 2007). Making the side-chains

more rigid might be expected to amplify these effects and lead to even more marked changes in hepatic metabolism. To test this expectation we have studied the three positional isomers **7–9** (Boiadjiev and Lightner, 2003) which differ constitutionally only in the lengths of the carbon chains connecting the carboxyl groups to the pyrrole rings. In **7–9** these carbon chains are the same length as those in the homologs **6b–d**, respectively. In this paper we show that **7–9**, despite their superficially similar linear representations, are metabolized very differently from each other and from the parent compound mesobilirubin XIII $\alpha$  (**6b**) with respect to glucuronidation and Mrp2-mediated transport into bile and we correlate their metabolism with their preferred conformations calculated previously by force-field molecular mechanics.

## Materials and Methods

Synthesis and characterization of **7**, **8** and **9** are described elsewhere (Boiadjiev and Lightner, 2003). Bilirubin ditaurate (**10**) was from Porphyrin Products (now Frontier Scientific), Logan, UT and di-*n*-octylamine from Aldrich. Animal procedures, sources of rats and HPLC methods were as detailed elsewhere (Woydziak et al., 2005; McDonagh and Lightner, 2007). For biliary excretion studies, pigments (~0.25 mg, accurately weighed), freshly dissolved in argon-degassed 0.1 M NaOH, were quantitatively diluted into 1 mL rat serum. The solution was microfuged briefly, two 20- $\mu$ L aliquots were taken from the supernate for HPLC and the remainder was injected intravenously over ~30 sec into the femoral vein of a male rat (>250 g) fitted with a short (7.5-cm) indwelling PE-50 biliary cannula for rapid collection of bile. Bile was collected in 20- $\mu$ L aliquots into glass tubes and flash-frozen immediately with dry ice. Frozen samples were stored at  $-70^{\circ}\text{C}$  pending HPLC analysis, when they were vortex-mixed with 80  $\mu$ L 0.1 M di-*n*-octylamine acetate (prepared from di-*n*-octylamine and glacial acetic acid) in MeOH (MeDocta) and microfuged. A 50- $\mu$ L aliquot of the supernate was injected without delay via a 20- $\mu$ L sample loop into the HPLC instrument and eluting peaks detected at or close to the absorption maximum of the compound being studied ( $\lambda_{\text{max}}$  for **7**, **8**, and **9** in the HPLC eluent: 428, 398 and 396 nm respectively) and at 450 nm, the absorption maximum for bilirubin. The isocratic HPLC eluent used throughout was MeDocta containing from 0–8% water. The column was a Beckman-Altex Ultrasphere-IP 5  $\mu$ m C-18 ODS column (25  $\times$  0.46 cm), maintained at 37–40 $^{\circ}\text{C}$ , fitted with a similarly-packed precolumn (4.5  $\times$  0.46 cm) connected to a Hewlett-Packard multi-wavelength diode array detector. Biliary excretion curves were derived by plotting HPLC peak areas (measured with HP ChemStation software) normalized to the maximum peak area. The fraction of the injected dose excreted was estimated by comparing the area under the biliary excretion curve (HPLC peak area versus time), adjusted for total bile volume excreted, with the HPLC peak area of the pigment in a 20- $\mu$ L sample of the original serum solution injected into the rat. Areas under biliary excretion curves were determined using Un-Scan-It software (Silk Scientific, Inc.,

Orem, Utah). Molecular models are based on coordinates generated by Sybyl molecular dynamics calculations (except for models of bilirubin IX $\alpha$  which are based on published X-ray crystal coordinates; Bonnet et al., 1978) and were drawn using CrystalMaker (Version 6.3.10 for Mac OS-X, CrystalMaker Software Ltd., Yarnton, UK). For generation of photoisomers of **7**, 1.6 mg was dissolved in 10 ml CHCl<sub>3</sub>/Et<sub>3</sub>N (1:1) in a 10-ml Erlenmeyer flask and the solution purged with argon. With continued argon bubbling, the flask was placed on a horizontal 20-W Westinghouse Special Blue F20T12/BB fluorescent tube with maximum output at ~430–460 nm and irradiated for 10 min to generate a photostationary mixture of photoisomers. [Not having sufficient material for detailed wavelength dependence studies, we based the irradiation time on similar experiments with bilirubin. Because the photoisomerization is reversible, prolonged irradiation does not necessarily generate a higher yield of photoisomers and may lead to decomposition products.] The solution was flash-evaporated on a rotary evaporator and the residue further dried at room temperature under vacuum (<1mm Hg). This preparation was repeated with 1.1 mg **7**. The residue from the first preparation was rinsed with 1.5 ml rat serum in two portions and the combined rinses microfuged. The supernate was used to similarly rinse the residue from the second preparation. Samples of this solution were taken for HPLC (**Fig 6**) and the remainder divided into two equal portions which were used for excretion studies in one Gunn and one wild-type (Sprague-Dawley) rat respectively (**Fig 8**). Except for photochemical procedures, all procedures involving pigment solutions, bile samples and bile collection were done under red or orange safelights in a dark-room.



## Results

The yellow di-*o*-benzoic acid rubin **7**, injected intravenously as a bolus dissolved in rat serum, was not excreted to any significant extent in bile in Gunn or wild-type rats over the 4-hr period of study. When **7** was irradiated briefly with blue light under argon in CHCl<sub>3</sub>/Et<sub>3</sub>N and the residue, after removal of solvent under vacuum, was dissolved in rat serum two new peaks appeared (**Fig 6**) on HPLC, one in only relatively small amounts, corresponding to more polar compounds. The absorption spectrum of the major photoproduct was similar to that of the parent compound **7**. Although the photoproducts were not characterized further, there is little doubt that the major new peak is the *E,Z* isomer of **7** (**Fig 7**) and the minor peak the *E,E* isomer (Lightner et al., 1979; McDonagh et al., 1979; McDonagh et al., 1982). When the serum solution was injected i.v. into a normal rat (**Fig 8**) or a Gunn rat both photoisomers were excreted promptly in bile, accompanied by only traces of *Z,Z*-**7**.

In contrast to **7**, both the di-*m*- and di-*p*-benzoic isomers (**8** and **9**), were excreted quantitatively in bile in both Gunn rats and normal rats within two hr, and in normal rats there was no evidence for glucuronide formation (**Fig 9**). Excretion was rapid with the concentration of unchanged injected rubin in bile peaking <6–9 min after injection, of which several min represents external flow through the biliary cannula.

Although **8** and **9** showed similar rates of biliary excretion in Gunn and normal rats, their excretion differed markedly in mutant rats (Jansen et al., 1985; Jansen et al., 1993) congenitally deficient in Mrp2 (TR<sup>-</sup> rats) (**Fig 10**). The di-*m*-benzoic isomer (**8**) was excreted rapidly; 0.60 ± 0.12 of the administered dose was excreted in bile within 2 hr. In contrast, the di-*p*-benzoic isomer (**9**) was excreted to a very minor extent characterized by slow steady excretion of a low concentration of unchanged pigment throughout the experiment.

Previous studies have shown that the ditaurine conjugate of bilirubin (**10**) does not depend on Mrp2 for efficient elimination in bile (Jansen et al., 1993). To compare the rate of excretion of the di-*m*-benzoic isomer (**8**) with that of bilirubin ditaurine amide a mixture of the two pigments was injected into TR<sup>-</sup> rats and the rate of biliary excretion of both pigments compared. The two pigments were excreted at essentially identical rates (*Fig 10d*).

## Discussion

Their high affinity for serum albumin notwithstanding, bilirubin (**1**) and mesobilirubin XIII $\alpha$  (**6b**) are cleared rapidly from plasma by hepatic uptake when injected intravenously as small bolus doses in the rat. The mechanism of uptake is uncertain, both active and passive transport mechanisms having been proposed (Zucker and Goessling, 2000; Cui et al., 2001; Wang et al., 2003). Although both are dipropanoic acids, which are usually ionized at physiologic pH, they are not allocrites for any of the transporters in the canalicular membrane of the liver and are not excreted significantly in unchanged form in bile. This contrasts with the constitutionally very similar biliverdins (dehydro-bilirubins, e.g. **2**) which are excreted rapidly in unchanged form, provided that they are not reduced by biliverdin reductases (McDonagh et al., 2002). The anomalous behaviour and the surprising lipophilicity of bilirubin have been ascribed to its preference for conformations in which the polar carboxyl (carboxylate), amino and lactam functions are sequestered within the molecule by intramolecular hydrogen bonding, thereby shielding them from aqueous solvation. According to this theory, strengthening, relaxing or preventing the intramolecular hydrogen bonding should have profound effects on metabolism. This is strikingly borne out by the observations in this paper which are summarized in Table 1 along with some relevant earlier findings.

Each of the three constitutionally similar isomers **7**, **8** and **9** is metabolized quite differently in the rat. They are also metabolized differently from the corresponding alkanolic congeners **6b,c** and **d** and in ways that are different from what might be intuitively expected on the basis of the usual linear representations shown in Table 1. For example, comparing **6c** and **8**, the presence of the extra aromatic functionality in **8** would not be expected to facilitate its hepatobiliary excretion and obviate the need for Phase 2 metabolism, particularly acyl glucuronidation.

The results become more explicable when the preferred three-dimensional structures of the molecules, deduced from molecular mechanics calculations, are considered (Boiadjev and Lightner, 2003). Although the energy-minimizations refer to the gas-phase, adjusted to solvent dielectric, there is abundant evidence that the calculated structures closely reflect crystal and solution structures. The energy-minimized conformation of **7** is shown in **Fig 12** in space-filled and stick representations. The structure is reminiscent of the hydrogen-bonded ridge-tile structures of bilirubin and mesobilirubin with the lipophilic edges of the two phenyl rings protruding from the ridge of the tile. The *o*-carboxyl groups are favorably positioned for intramolecular hydrogen bonding with NHCO and NH functions as in bilirubin (**1**) or mesobilirubin XIII $\alpha$  (**6b**) and the greater acidity of the aromatic COOHs relative to an aliphatic COOHs may strengthen the hydrogen-bonding in **7** compared to that in **1** or **6b**. More importantly, steric interactions between pyrrole methyl groups and proximate phenyl rings (indicated by double-headed arrows in **Fig 12**) force the phenyl rings to twist in such a way as to lock in and stabilize the hydrogen bonding. The resulting lipophilic structure accounts for **7**'s much longer elution time on reverse-phase HPLC compared to bilirubin (**Fig 13**) and its failure to be excreted in bile in the Gunn rat. In contrast to bilirubin and mesobilirubin XIII $\alpha$ , **7** is not glucuronidated by UGT1A1 or other hepatic UGT enzymes in vivo. We speculate that this is because the buttressing effect of the rotationally-restricted planar phenyl rings hinders opening and acylation of the hydrogen-bonded carboxyl groups at the UGT1A1 active site. Consistent with this explanation, *E,Z* and *E,E* photoisomers of **7** (**Fig 7**), in which intramolecular hydrogen bonding of one or both of the carboxylic acid groups, respectively, is sterically impossible, were excreted rapidly and unchanged in bile in the Gunn rat, unlike the fully hydrogen-bonded *Z,Z* isomer (**Fig 8**). The resistance of **7** to hepatobiliary excretion and glucuronidation is reminiscent of the behavior of the bisacetylenic compound **11**, an almost planar molecule with compact intramolecular hydrogen bonding of its carboxyl groups. As with **7**, the *E,Z* isomer of **11**, but not the *Z,Z* isomer, was excreted without conjugation in the Gunn rat (McDonagh and Lightner, 2007).

Consistent with the proposed effect of intramolecular hydrogen bonding and in marked contrast to **7**, the corresponding *m*- and *p*- isomers were excreted rapidly and unchanged in bile in both Gunn and wild-type rats. In the *m*- and *p*- isomers (**8** and **9**) intramolecular steric interactions of the bulky phenyl groups force the dipyrinone chromophores out of planarity and “lock” the carboxyl groups into orientations in which they protrude from the molecular surface and intramolecular hydrogen bonding is precluded (**Fig 15**). This accounts for their relatively short retention times on HPLC compared to bilirubin and the *o*- isomer **7** (**Fig 13**), both pigments being eluted close to bilirubin monoglucuronides. Surprisingly, however, the *m*- and *p*- isomers behaved differently when tested in TR<sup>-</sup> rats (**Fig 10**), which lack the canalicular transporter Mrp2. The biliary excretion of the most polar *p*- isomer (**9**) was markedly retarded compared to its excretion in Gunn and normal rats, indicating that Mrp2 is essential for its efficient biliary excretion in these animals. In contrast, the *m*- isomer (**8**) was excreted promptly and unchanged even in TR<sup>-</sup> rats. When injected in tandem with bilirubin ditaurine amide (**10**), which is known not to depend on Mrp2 for excretion into bile, the two pigments were excreted at similar rates (**Fig 10d**). Thus, of the two isomers **8** and **9**, only one, the *p*- isomer, is strongly dependent on Mrp2 for efficient biliary excretion. This difference is surprising in view of their similar structures.

Previous studies have shown that **7** and **8** exhibit atropisomerism (Boiadjev and Lightner, 2002), depicted in Figure 16 for **7**. For **7**, the predominant isomer is **7-anti** in which there is compact intramolecular hydrogen bonding of both COOH groups. In some solvents this isomer is accompanied by a smaller proportion of the **7-syn** atropisomer (**Fig 16**) in which one of the phenyl rings has been rotated through 180°, thus exposing the attached COOH and preventing it from engaging in intramolecular hydrogen bonding with pyrrolic NH and NH/CO groups. This atropisomer would be expected to be more polar than the corresponding **7-anti** isomer and more readily excretable in bile. The fact that **7** was not excreted promptly suggests that little, if any, of the **7-syn** atropisomer was present in the injectate. However, the weak biliary excretion that was observed might be attributable to the presence of a very

small proportion. The *m*-benzoic isomer **8** can also undergo atropisomerism, but in this case all of the atropisomers have exposed COOH groups and would be expected to exhibit similar hepatobiliary metabolism.

Our results show that two-dimensional constitutional representations of molecules can be misleading when predicting their hepatobiliary metabolism. They also show how effects of steric compression, relayed through conformational changes, can markedly influence intramolecular hydrogen bonding and hepatic metabolism. For the isomers in this study, reinforcing hydrogen bonding by steric compression inhibits hepatobiliary excretion, whereas prevention of hydrogen bonding allows the molecules to slip past hepatic UGT enzymes and, in one case, to traverse the canalicular membrane even in the absence of the transporter Mrp2. Extrapolating from rats to humans is difficult given the species differences in the substrate affinities of enzymes and drug transport proteins. However, the same general principles should apply. A striking example is in phototherapy of neonatal jaundice (Maisels and McDonagh, 2008) where photochemically-induced isomerization and disruption of the hydrogen bonding in bilirubin facilitates excretion of the pigment in bile in unconjugated form (Lightner and McDonagh, 1984). The same general process occurs in jaundiced rats (Gunn rats) on exposure to light, but because of differences in protein binding the excretion kinetics of the photoisomers are different in rats and humans (Ennever et al., 1985, 1987; Lightner and McDonagh, 1984).

**Acknowledgements.**

We thank Wilma Norona for technical assistance.

## References

- Boiadjiev SE and Lightner DA (2002) Atropisomerism in linear tetrapyrroles. *Tetrahedron* **58**:7411–7421.
- Boiadjiev SE and Lightner DA (2003) Novel benzoic acid congeners of bilirubin. *J Org Chem* **68**:7591–7604.
- Bonnett R, Davies JE, Hursthouse MB and Sheldrick GM (1978) The structure of bilirubin. *Proc Roy Soc Lond B* **202**:249–268.
- Cui Y, König J, Leier I, Buchholz U and Keppler D (2001) Hepatic uptake of bilirubin and its conjugates by the human organic anion transporter SLC21A6. *J Biol Chem* **276**:9626–9630.
- Ennever JF, Knox I, Denne SC and Speck WT (1985) Phototherapy for neonatal jaundice: in vivo clearance of bilirubin photoproducts. *Pediatr Res* **19**:205–208.
- Ennever JF, Costarino AT, Polin RA and Speck WT (1987) Rapid clearance of a structural isomer of bilirubin during phototherapy. *J Clin Invest* **79**:1674–1678.
- Harrop GA and Barron ESG (1931) The excretion of intravenously injected bilirubin as a test of liver function. *J Clin Invest* **9**:577–587.
- Jansen PL, Peters WH and Lamers WH (1985) Hereditary chronic conjugated hyperbilirubinemia in mutant rats caused by defective hepatic anion transport. *Hepatology* **5**:573–579.
- Jansen PLM, Vanklinken JW, Vangelder M, Ottenhoff R and Oude Elferink RPJ (1993) Preserved organic anion transport in mutant TR<sup>-</sup> rats with a hepatobiliary secretion defect. *Am J Physiol* **265**:G445–G452.
- Kaplan M and Hammerman C (2005) Bilirubin and the genome: The hereditary basis of unconjugated neonatal hyperbilirubinemia. *Current Pharmacogenomics* **3**:21–42.
- Kornberg A (1942) Latent liver disease in persons recovered from catarrhal jaundice and in otherwise normal medical students as revealed by the bilirubin excretion test. *J Clin Invest* **21**:299–308.



- Lightner DA and McDonagh AF (1984) Molecular mechanisms of phototherapy for neonatal jaundice. *Acc Chem Res* **17**:417–424.
- Lightner DA, Wooldridge TA and McDonagh AF (1979) Configurational isomerization of bilirubin and the mechanism of jaundice phototherapy. *Biochem Biophys Res Commun* **86**:235–243.
- Maisels MJ and McDonagh AF (2008, In press) Phototherapy for the treatment of neonatal jaundice. *NEJM*.
- McDonagh AF (1990) Is bilirubin good for you? *Clin Perinatol* **17**:359–369.
- McDonagh AF and Lightner DA (1991) The importance of molecular structure in bilirubin metabolism and excretion, in: *Hepatic Metabolism and Disposition of Endo- Xenobiotics* (Bock KW, Gerok W, Matern S and Schmid R eds), pp 47–59, Kluwer, Dordrecht.
- McDonagh AF and Lightner DA (2007) Influence of conformation and intramolecular hydrogen bonding on the acyl glucuronidation and biliary excretion of acetylenic bis-dipyrrinones related to bilirubin. *J Med Chem* **50**:480–488.
- McDonagh AF, Lightner DA, Kar AK and Norona WS (2002) Hepatobiliary excretion of biliverdin isomers and C10-substituted biliverdins in Mrp2-deficient (TR<sup>-</sup>) rats. *Biochem Biophys Res Commun* **293**:1077–1083.
- McDonagh AF, Lightner DA, Nogales DF and Norona WS (2001) Biliary excretion of a stretched bilirubin in UGT1A1-deficient (Gunn) and Mrp2-deficient (TR<sup>-</sup>) rats. *FEBS Lett* **506**:211–215.
- McDonagh AF, Lightner DA and Wooldridge TA (1979) Geometric isomerization of bilirubin IX $\alpha$  and its dimethyl ester. *J Chem Soc Chem Commun* 110.
- McDonagh AF, Palma LA, Trull FR and Lightner DA (1982) Phototherapy for neonatal jaundice. Configurational isomers of bilirubin. *J Am Chem Soc* **104**:6865–6867.
- Nies AT and Keppler D (2007) The apical conjugate efflux pump ABCC2 (MRP2). *Pflugers Arch* **453**:643–659.

- Ollinger R, Wang H, Yamashita K, Wegiel B, Thomas M, Margreiter R and Bach FH (2007a) Therapeutic applications of bilirubin and biliverdin in transplantation. *Antioxid Redox Signal* **9**:2175–2186.
- Ollinger R, Yamashita K, Bilban M, Erat A, Kogler P, Thomas M, Csizmadia E, Usheva A, Margreiter R and Bach FH (2007b) Bilirubin and biliverdin treatment of atherosclerotic diseases. *Cell Cycle* **6**:39–43.
- Owens IS, Basu NK and Banerjee R (2005) UDP-glucuronosyltransferases: gene structures of UGT1 and UGT2 families. *Methods Enzymol.* **400**:1–22.
- Person RV, Peterson BR and Lightner DA (1994) Bilirubin conformational analysis and circular dichroism. *J Am Chem Soc* **116**:42–59.
- Smith PC, McDonagh AF and Benet LZ (1986) The irreversible binding of zomepirac to plasma protein in vitro and in vivo. *J Clin Invest* **77**:934–939.
- Stocker R (2004) Antioxidant activities of bile pigments. *Antioxid Redox Signal* **6**:841–849.
- Stocker R, Yamamoto Y, McDonagh AF, Glazer AN and Ames BN (1987) Bilirubin is an antioxidant of possible physiological importance. *Science* **235**:1043–1046.
- Trull FR, Person RV and Lightner DA (1997) Conformational analysis of symmetric bilirubin analogues with varying length alkanolic acids. Enantioselectivity by human serum albumin. *J Chem Soc, Perkin Trans 2*:1241–1250.
- Wang P, Kim RB, Chowdhury JR and Wolkoff AW (2003) The human organic anion transport protein SLC21A6 is not sufficient for bilirubin transport. *J Biol Chem* **278**:20695–20699.
- Woydziak ZR, Boiadjev SE, Norona WS, McDonagh AF and Lightner DA (2005) Synthesis and hepatic transport of strongly fluorescent cholephilic dipyrinones. *J Org Chem* **70**:8417–8423.
- Zucker SD and Goessling W (2000) Mechanism of hepatocellular uptake of albumin-bound bilirubin. *Biochim Biophys Acta* **1463**:197–208.

**Footnotes**

- a) Supported by NIH grants HD-17779 and DK-26307.
- b) Reprint requests should be addressed to:  
Antony F. McDonagh  
Division of Gastroenterology  
University of California San Francisco  
Room S-357, Box 0538  
513 Parnassus Avenue  
San Francisco, CA 94143-0538  
Email: [tony.mcdonagh@ucsf.edu](mailto:tony.mcdonagh@ucsf.edu)
- c) Dedicated to Professor Leslie Z. Benet on the occasion of his 70th birthday and to the memory of Professor Emeritus Rudi Schmid who died on October 20, 2007 aged 85.

## Figure Legends

FIG. 1. Constitutional structure and numbering system of bilirubin IX $\alpha$ . The 4,5 and 15,16 carbon-carbon double bonds have the *Z* configuration, as opposed to the *E*.

FIG. 2. Space-filling and stick representations of the preferred conformation of bilirubin **1** in two different orientations. Striped bonds represent hydrogen bonds.

FIG. 3. Constitutional structures of compounds **2-5**.

FIG. 4. Constitutional structures of compounds **6a-6e**.

FIG. 5. Constitutional structures of compounds **6b-6d** and **7-9**. The heavy bonds show common carboxylic acid connectivities in each left/right pair of structures.

FIG. 6. (*Left*) HPLC of **7** after irradiation in CHCl<sub>3</sub>/Et<sub>3</sub>N and dissolution of the isomer mixture in rat serum. HPLC eluent MeDocta/0% water. The inset shows an HPLC of unirradiated **7** in rat serum. (*Right*) Normalized absorbance spectra of **7** (dotted line) and the putative *Z,E* photoisomer of **7** (solid line).

FIG. 7. Photoisomerization of **7** (a third *E,E* isomer is not shown).

FIG. 8. Excretion of photoisomers of **7** in a normal rat. The lower HPLC is of the mixture of photoisomers in rat serum injected into the rat. The middle HPLC is of bile from the rat before injection. BDG and BMG stand for bilirubin diglucuronide and bilirubin monoglucuronide respectively. The top HPLC is of bile 12 min after injection. Similar excretion of only the photoisomers was also observed in the Gunn rat. HPLC eluent MeDocta/0% water.

FIG. 9. Excretion of *m*- and *p*-benzoic isomers **8** and **9** in Gunn and normal rats. **a**. Biliary excretion profiles for **8** in normal (filled circles) and Gunn (open circles) rats. **b**. Biliary excretion profiles for **9** in normal (filled circles) and Gunn (open circles). (Plots in **a** and **b** are means of duplicate experiments). **c,e**. HPLC chromatograms of bile before and after injection of **8** in Gunn (**c**) and normal (**e**) rats. Eluent MeDocta/5% water. **d,f**. Chromatograms of bile before and after injection of **9** in Gunn (**d**) and normal (**f**) rats. Eluent MeDocta/8% water.

FIG. 10. *Top*. HPLC of bile before and 15 min after injecting **8** (panel **a**) and **9** (panel **b**) in TR<sup>-</sup> rats. *Bottom*. Panel **c**. Profile for biliary elimination of **8** in TR<sup>-</sup> rats (mean  $\pm$  SD of 7 experiments). Panel **d**. Biliary excretion profiles for **8** and bilirubin ditaurine amide (**10**) after simultaneous injection into TR<sup>-</sup> rats. Open circles, **10**. Closed circles, **8**. Curves are means of duplicate experiments. HPLC mobile phases as in Figure 9.

FIG. 11. Constitutional structure of the ditaurine conjugate disodium salt of bilirubin.

FIG. 12. Space-filling and stick representations of the preferred hydrogen-bonded conformation of *o*-benzoic isomer **7** in two orientations. Striped bonds represent hydrogen bonds.

FIG. 13. HPLC of a mixture of bilirubin and the *p*-, *m*-, and *o*-isomers **9**, **8** and **7**. HPLC eluent, MeDocta/2% water.

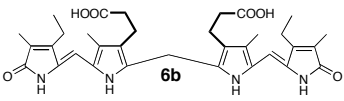
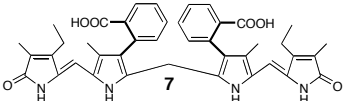
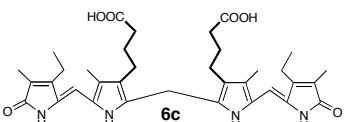
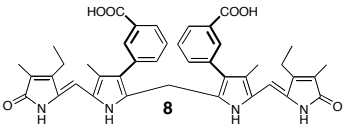
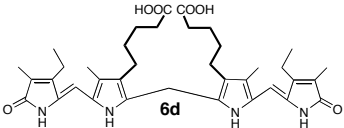
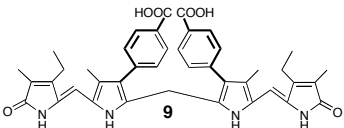
FIG. 14. Hydrogen-bonded structure of exploded bilirubin **11**.

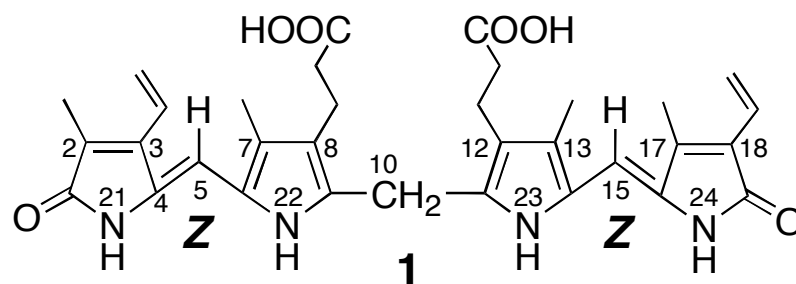
FIG. 15. Stick representations of the preferred conformations of (*left*) *m*-benzoic isomer **8** and (*right*) *p*-benzoic isomer **9**.

FIG. 16. Atropisomers of **7**.

TABLE 1

*Comparison of the biliary excretion of benzoic substituted isomers 7–9 and their fully aliphatic counterparts 6b–6d. Based on observations in this paper and in (McDonagh and Lightner, 2007). Rapid biliary excretion means >60% of the injected dose excreted in <2 hrs with peak excretion <20 min after injection.*

| Compound  | Rapid biliary excretion |   |                         |
|---|-------------------------|---|-------------------------|
|   | Gunn (-UGT1)            | Normal (+UGT1)                          | TR <sup>-</sup> (-Mrp2) |
|    | No                      | Yes; as acyl glucuronides               | No                      |
|    | No                      | No                                      | No                      |
|    | No                      | Yes; as acyl glucuronides               | No                      |
|    | Yes                     | Yes                                     | Yes                     |
|   | Yes                     | Yes; unchanged and as acyl glucuronides | No                      |
|  | Yes                     | Yes                                     | No                      |



**Figure 1**

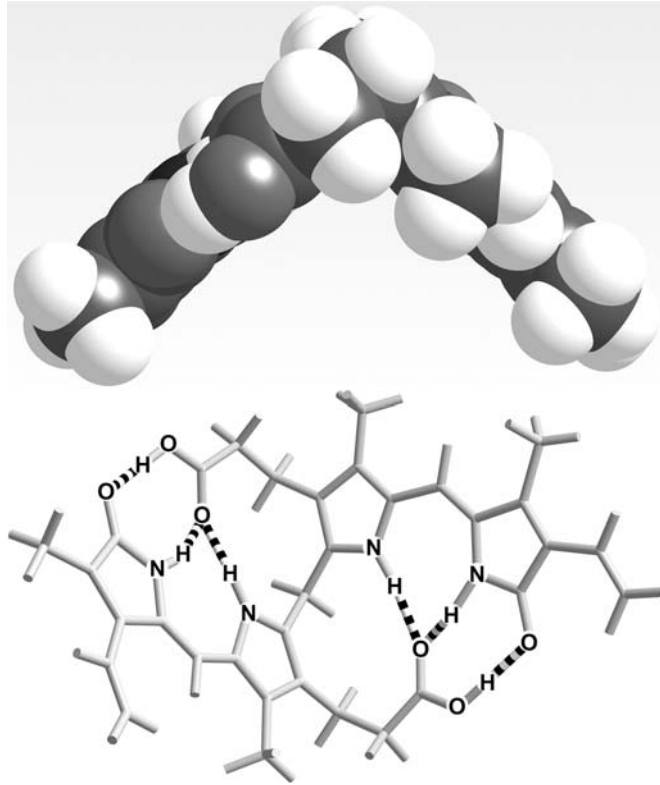


**Figure 2**



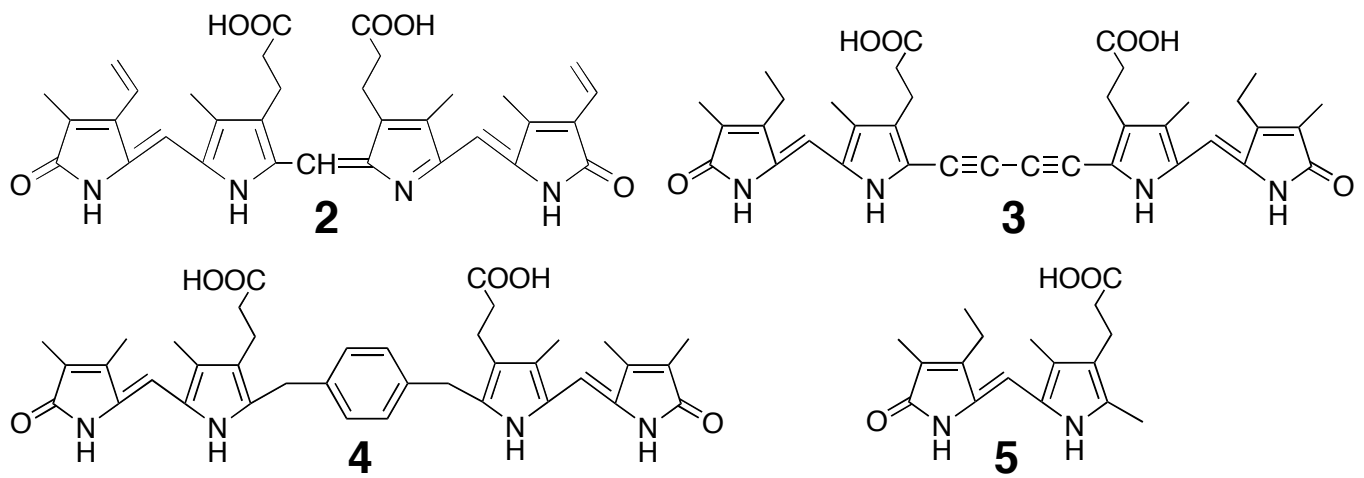


**Figure 3**

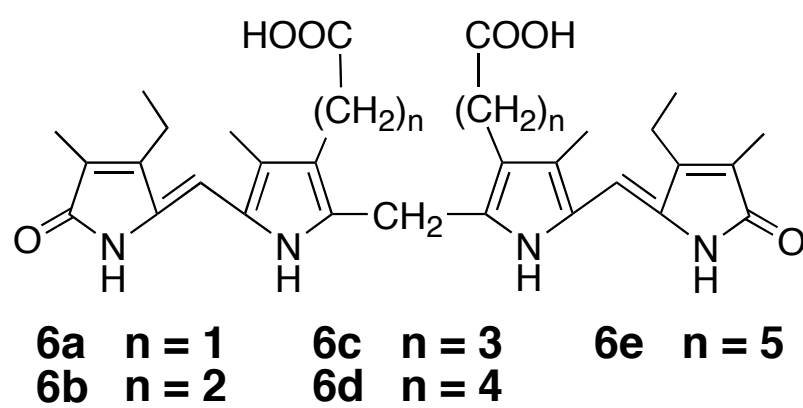


**Figure 4**

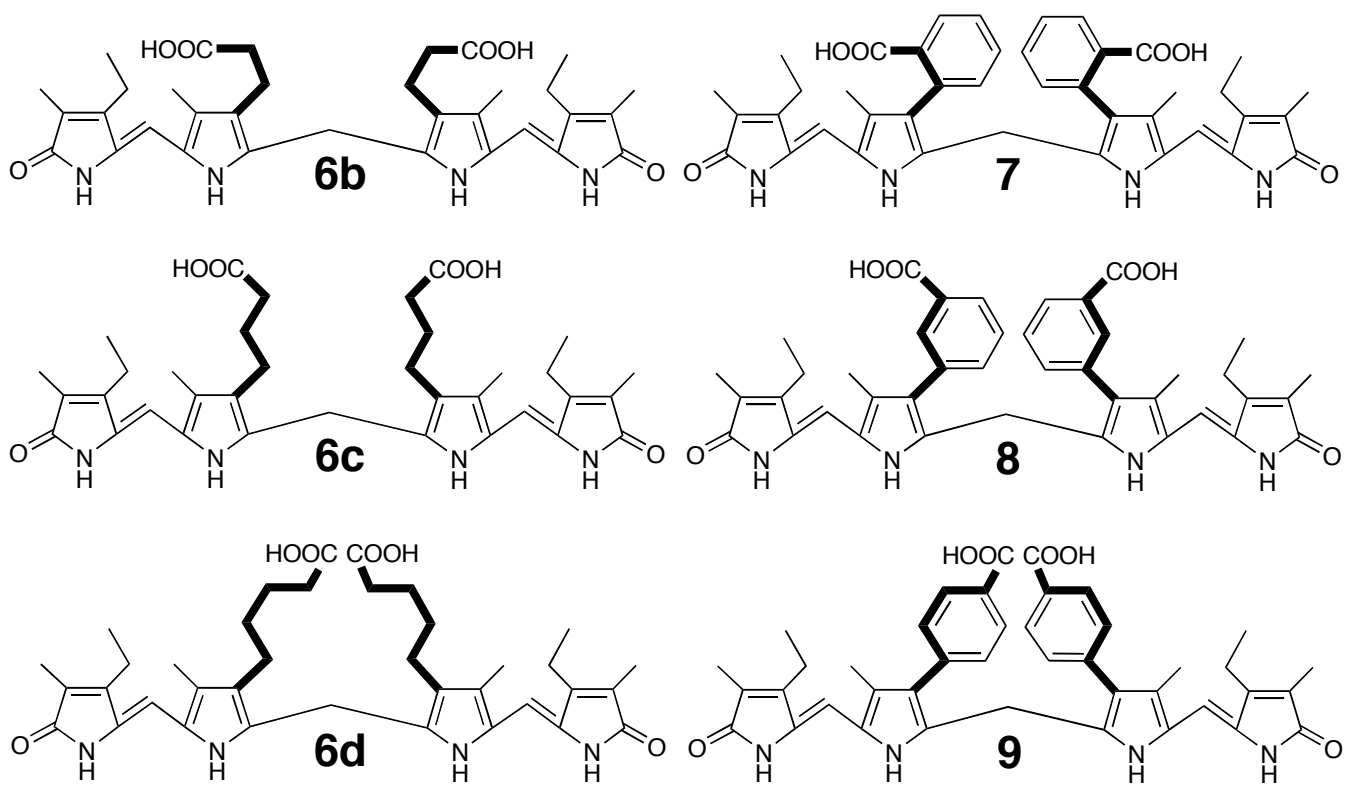


Figure 5

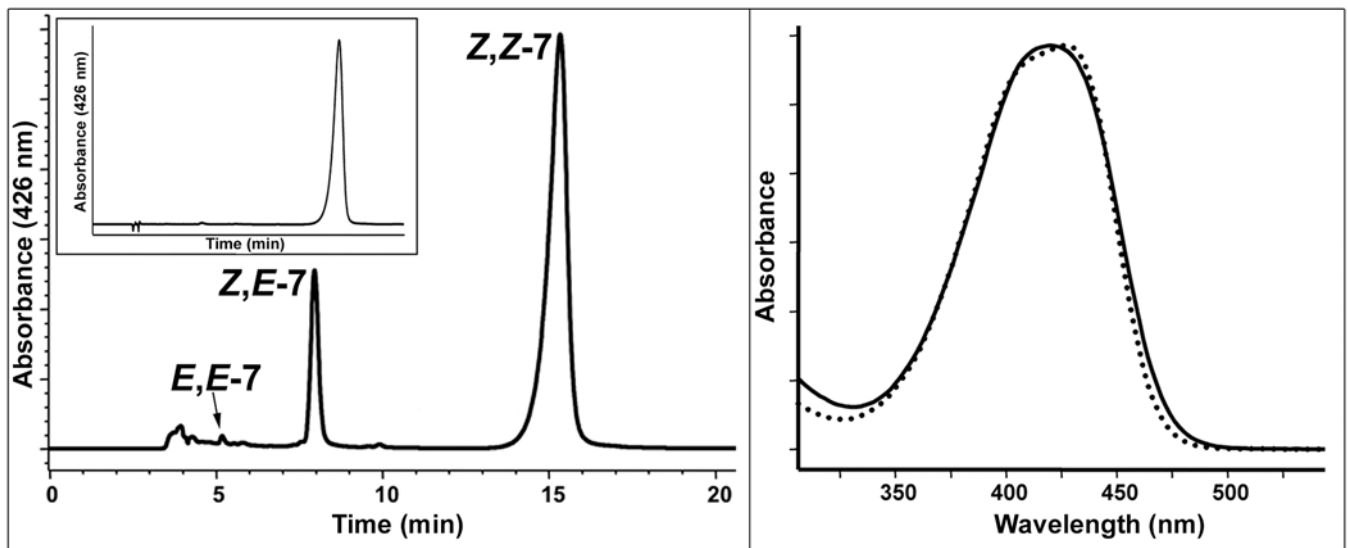
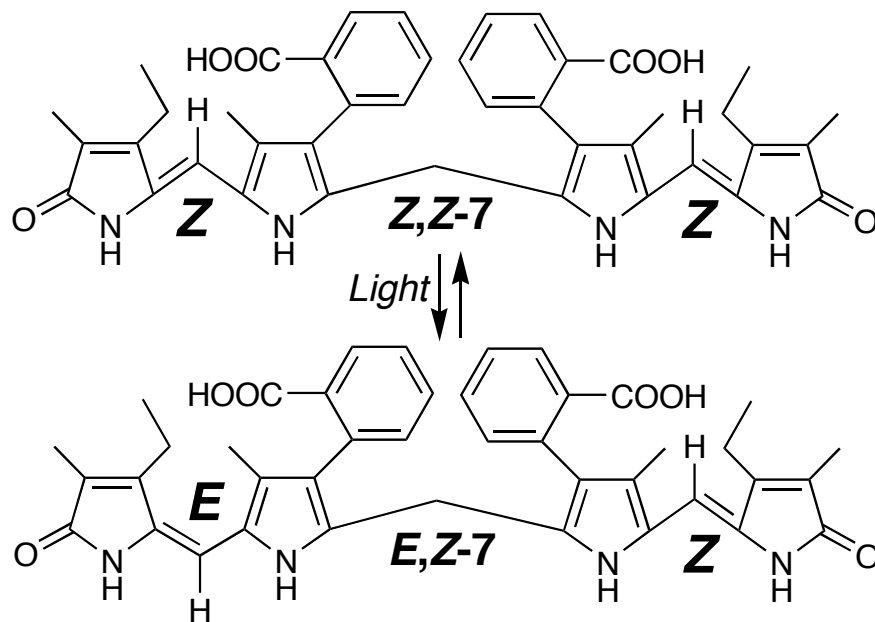


Figure 6



**Figure 7**

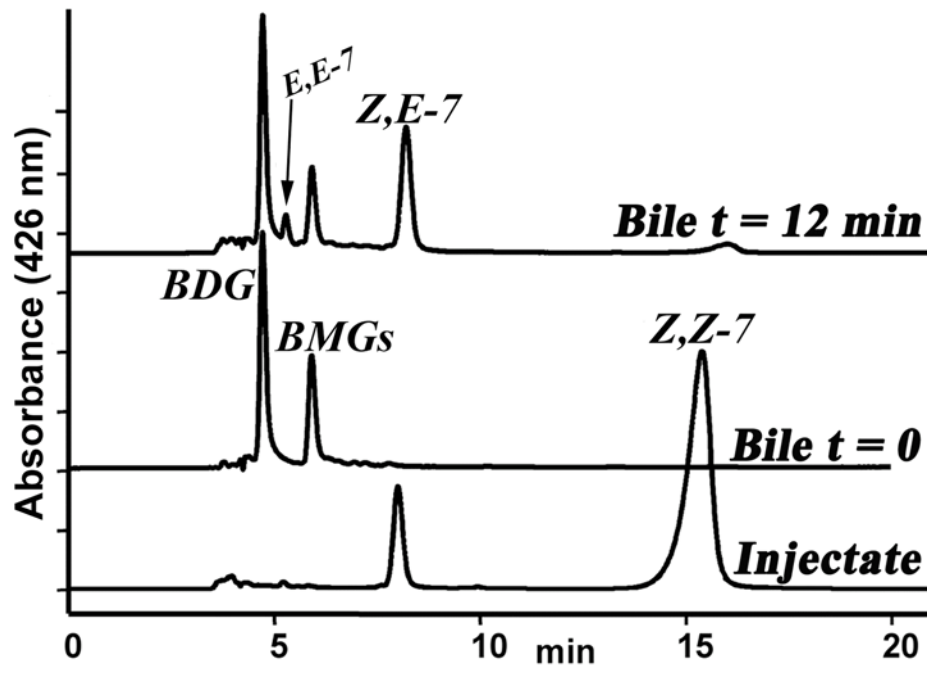


Figure 8

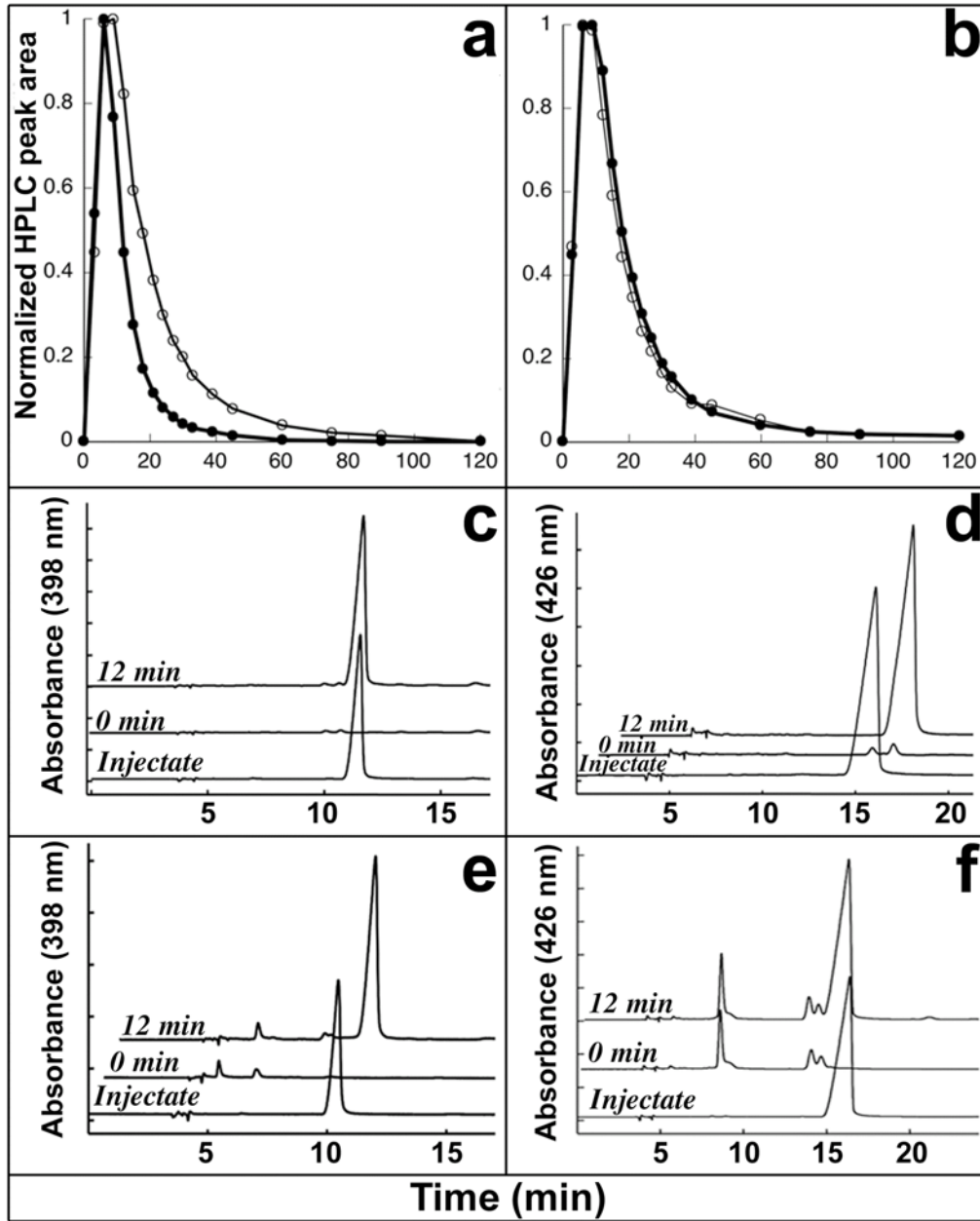


Figure 9

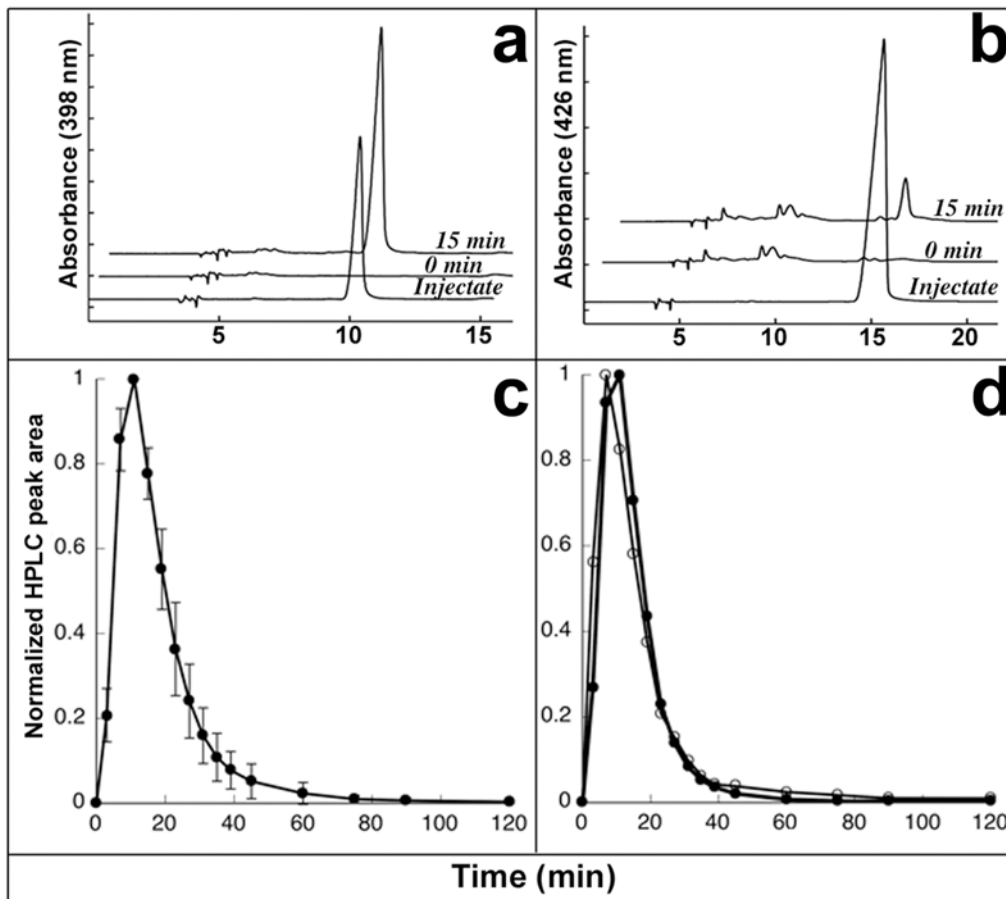
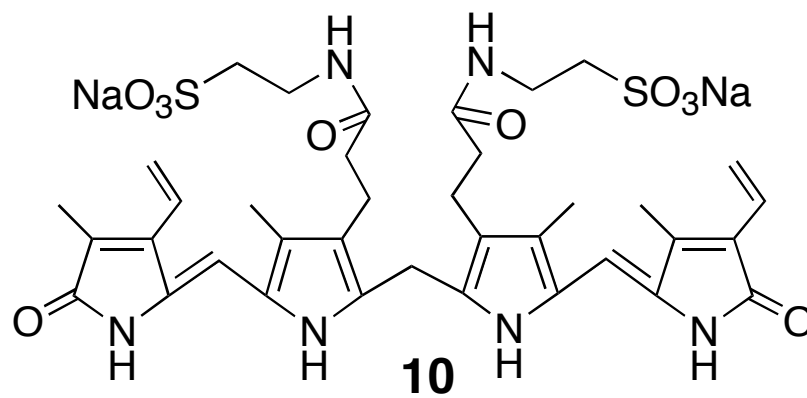
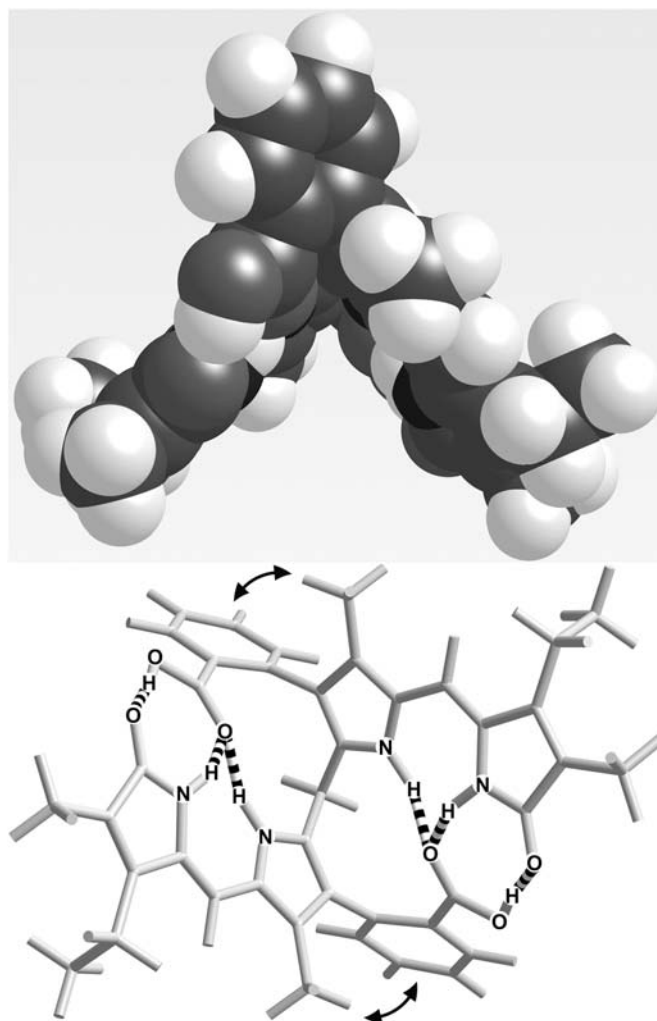


Figure 10





**Figure 11**



**Figure 12**

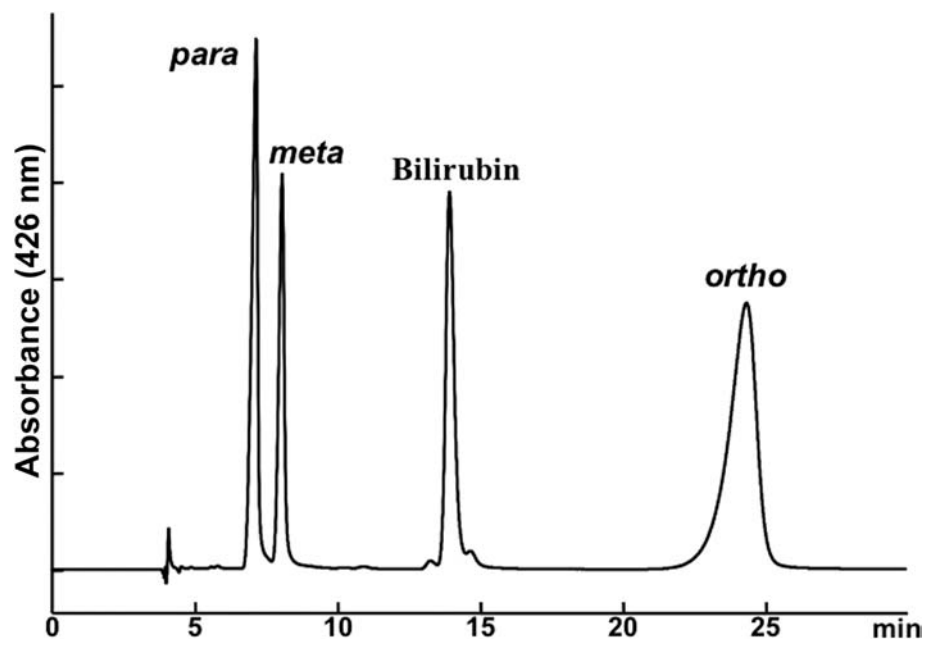


**Figure 13**

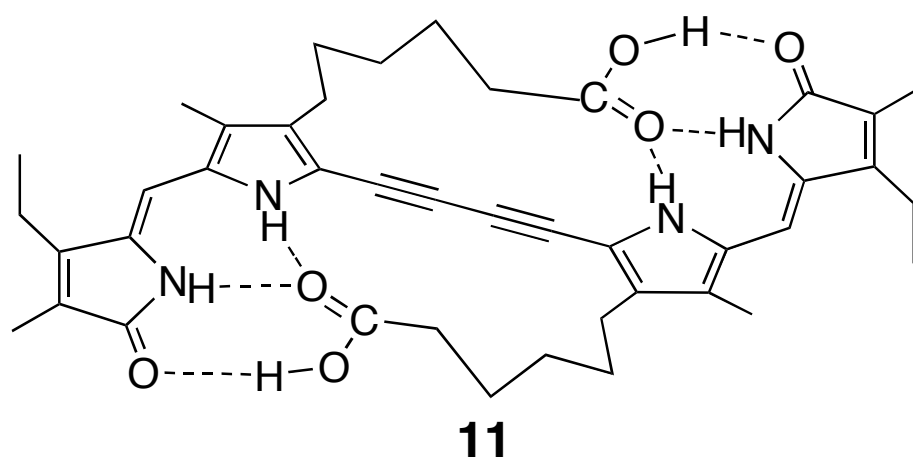


**Figure 14**

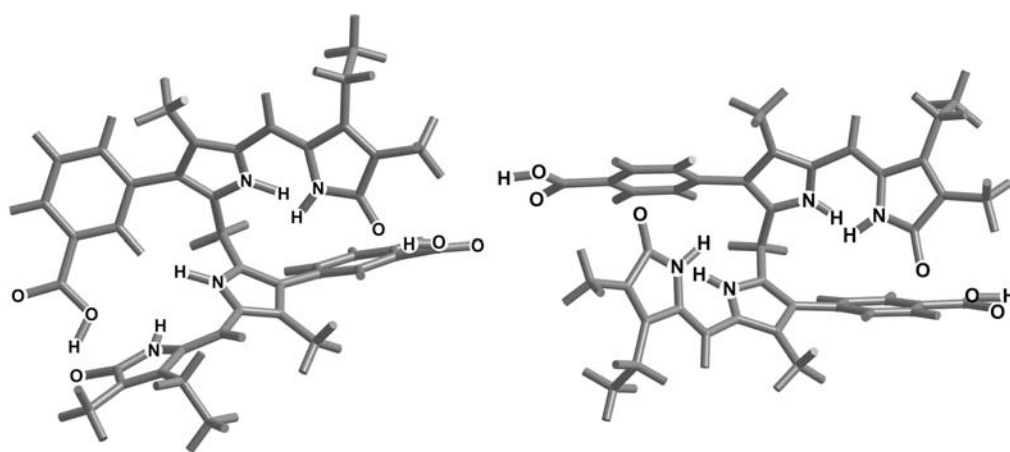


**Figure 15**

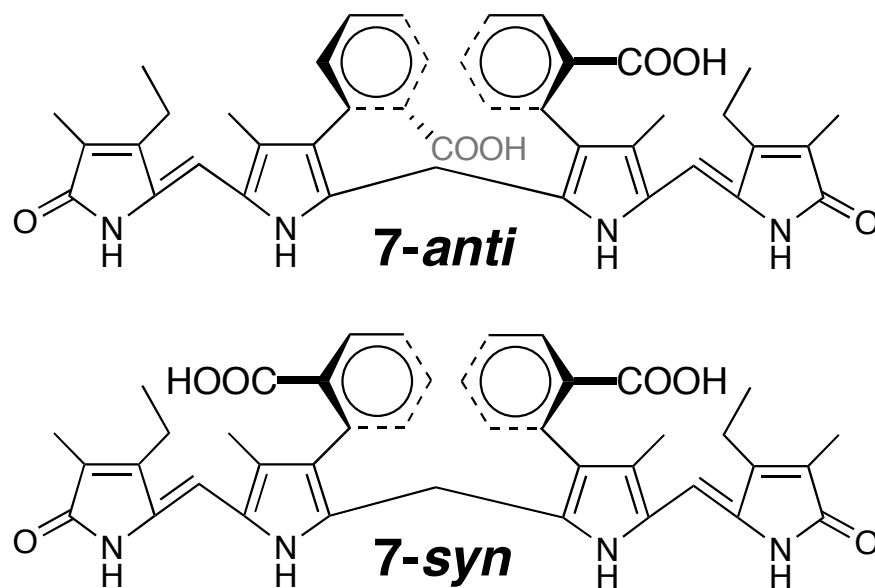


**Figure 16**